

Enhancement of retinal Müller glia's phagocytic activity against hard exudates by conbercept *via* activation of PPAR γ -CD36 axis in diabetic retinopathy

Ying-Ying Zhu¹, Shi-Yue Qin^{2,3}, Hai Xie⁴, Yin-Ping Liu¹, Xiao-Sa Li⁴, Chao-Yang Zhang^{5,6,7}, Yan-Chun Zhang⁸, Jing-Fa Zhang^{5,6,7}

¹Department of Ophthalmology, Yijishan Hospital, the First Affiliated Hospital of Wannan Medical College, Wuhu 241001, Anhui Province, China

²Department of Ophthalmology, Taizhou People's Hospital, Taizhou 225300, Jiangsu Province, China

³Department of Ophthalmology, the Second Affiliated Hospital of Soochow University, Suzhou 215004, Jiangsu Province, China

⁴Department of Ophthalmology, Shanghai General Hospital (Shanghai First People's Hospital), Shanghai Jiao Tong University School of Medicine, Shanghai 200025, China

⁵The Primasia International Eye Research Institute of the Chinese University of Hong Kong (Shenzhen), Shenzhen 518000, Guangdong Province, China

⁶C-MER (Shenzhen) Dennis Lam Eye Hospital, Shenzhen 518000, Guangdong Province, China

⁷C-MER Dennis Lam & Partners Eye Center, C-MER International Eye Care Group, Hong Kong 03309, China

⁸Department of Ophthalmology, Shaanxi Eye Hospital, Xi'an People's Hospital (Xi'an Fourth Hospital), Affiliated People's Hospital of Northwest University, Xi'an 710000, Shaanxi Province, China

Co-first Authors: Ying-Ying Zhu and Shi-Yue Qin

Correspondence to: Yan-Chun Zhang. Department of Ophthalmology, Shaanxi Eye Hospital, Xi'an People's Hospital (Xi'an Fourth Hospital), Affiliated People's Hospital of Northwest University, Xi'an 710000, Shaanxi Province, China. zhangyanchun1239@126.com; Jing-Fa Zhang. The Primasia International Eye Research Institute of the Chinese University of Hong Kong (Shenzhen), Shenzhen 518000, Guangdong Province, China. 13917311571@139.com

Received: 2025-01-07 Accepted: 2025-04-10

Abstract

• **AIM:** To investigate the effects and the underlying mechanism(s) of conbercept on the phagocytosis of hard exudates (HEs) by Müller glia in diabetic retinopathy (DR).

• **METHODS:** Twenty-one eyes from 17 patients with

diabetic macular edema (DME) underwent optical coherence tomography (OCT) imaging to examine the changes of HEs before and after intravitreal conbercept injection (IVC). *In vitro*, rat retinal Müller cell line (rMC-1) was cultured under high glucose and treated with oxidized low-density lipoprotein (Ox-LDL) with or without conbercept. Phagocytosis was analysed with immunofluorescence, flow cytometry, and Western blot. Expressions of scavenger receptors (LOX-1, CD36) were analyzed by quantitative real-time polymerase chain reaction (qRT-PCR). Conbercept's effects on vascular endothelial growth factor A (VEGF-A), VEGFR2, inflammation (NF- κ B, IL-6, iNOS), and oxidative stress (ROS) were evaluated with Western blot and immunofluorescence.

• **RESULTS:** The area of HEs showed minimal change after the first IVC (1.39 ± 1.41 to 1.38 ± 1.3 mm², $P=0.938$), but significantly decreased after the third IVC (0.45 ± 0.66 mm², $P=0.002$). *In vitro*, conbercept enhanced the phagocytosis of Ox-LDL by rMC-1 cells under high glucose condition. Conbercept reduced ROS and inflammation (NF- κ B, IL-6, iNOS) in high glucose-treated rMC-1 cells by suppression of VEGF/VEGFR2 pathway. The inhibition of NF- κ B by conbercept further activated PPAR γ -CD36 axis, increasing CD36 expression and promoting Ox-LDL uptake, thereby facilitating the clearance of HEs.

• **CONCLUSION:** Conbercept reduces HEs in DR by enhancing Müller glia phagocytosis possibly through activating PPAR γ -CD36 axis, which is mediated by inhibition of VEGF signaling. Modulation of Müller glia phagocytic capacity might provide a novel therapeutic strategy to treat DR and DME.

• **KEYWORDS:** conbercept; Müller glia; oxidized low-density lipoprotein; phagocytosis; vascular endothelial growth factor

DOI:10.18240/ijo.2025.07.07

Citation: Zhu YY, Qin SY, Xie H, Liu YP, Li XS, Zhang CY, Zhang YC, Zhang JF. Enhancement of retinal Müller glia's phagocytic activity against hard exudates by conbercept *via* activation of PPAR γ -CD36 axis in diabetic retinopathy. *Int J Ophthalmol* 2025;18(7):1252-1261

INTRODUCTION

Hard exudates (HEs) are lipid-rich deposits often observed in various retinal vascular diseases^[1], including diabetic retinopathy (DR), diabetic macular edema (DME), and retinal vein occlusion (RVO). The standard treatment for the above conditions is an intravitreal injection of anti-vascular endothelial growth factor (anti-VEGF) agents. Recent clinical studies have suggested that anti-VEGF treatment not only reduces macular edema but also diminishes HEs^[2-5], leading to speculation that these drugs might promote HEs absorption by modulation of retinal phagocytic cells.

Conbercept, a recombinant fusion protein with potent anti-VEGF activity, has shown efficacy in reducing retinal vascular leakage and improving visual outcomes^[6-7]. Although its primary mechanism of action is inhibiting VEGF-mediated vascular permeability and neovascularization, recent studies have indicated that conbercept might also exert different effects on retinal cells, such as enhancing the autophagy of retinal RF/6A cells^[8].

Retinal Müller cells, the predominant glial cells in the retina, play a crucial role in maintaining retinal homeostasis^[9]. Their cell bodies are primarily located in the inner nuclear layer (INL)^[10], which corresponds to the sites where HEs typically accumulate as observed on optical coherence tomography (OCT)^[11]. Müller cells exhibit phagocytic properties similar to those of macrophages. This phagocytic activity is essential for clearing cellular debris and metabolic waste, which helps to prevent the accumulation of HEs^[12-13]. The phagocytic function of retinal microglia has been extensively documented^[14-15], and there is growing interest among researchers regarding the phagocytic capacity of Müller glia in retinal metabolism. Previous studies have shown that Müller glia can eliminate degenerated photoreceptors before microglia intervention, a process modulated by phosphatidylserine and Rac1^[16]. Furthermore, in the absence of microglia, Müller glia can engulf other apoptotic cells in the retina, underscoring their significant phagocytic role^[17]. However, under diabetic condition, this phagocytic function of Müller glia might be compromised, thereby contributing to the accumulation of HEs. Currently, there is no report on the effect of conbercept on Müller glial phagocytosis. Additionally, *in vitro* evidence of this effect is lacking.

In this study, diabetic patients with DME were recruited to investigate the impact of conbercept on the clearance of HEs. Additionally, the phagocytic effects and potential mechanism(s) of Müller glia on oxidized low-density lipoprotein (Ox-LDL), treated with conbercept under diabetic condition, were explored *in vitro*.

PARTICIPANTS AND METHODS

Ethical Approval Twenty-one eyes from 17 treatment-

naïve patients with DR/DME were included and examined with the comprehensive ophthalmologic examinations at the Department of Ophthalmology, Yijishan Hospital affiliated to Wannan Medical College, Wuhu, China, between January 2022 and January 2024. This study was approved by the Clinical Research Ethical Committee of Wannan Medical College Yijishan Hospital (Approval No.2021-052) and adhered to the principles of the Declaration of Helsinki. All individual participants provided written informed consent.

Participants All patients underwent routine ophthalmic examinations, including best-corrected visual acuity, intraocular pressure, slit-lamp microscope and fundus examination, before and 1wk after intravitreal conbercept injection (IVC).

Inclusion criteria: 1) Diagnosis of type 2 diabetes mellitus; 2) Diagnosis of DR/DME; 3) Presence of HEs on fundus photography or hyperreflective foci with a size greater than 30 μm on OCT in macula.

Exclusion criteria: 1) History of previous anti-VEGF treatment or other ocular surgeries; 2) Retinal laser therapy within the past six months; 3) Presence of any other eye diseases that may cause HEs in the macula; 4) Coexistence of other eye conditions such as glaucoma, retinal detachment, and RVO that may lead to retinal pathology apart from DR; 5) Inability to obtain clear images due to media opacities such as cataract; 6) Unstable systemic condition or incomplete clinical data.

Intravitreal Conbercept Injection An experienced ophthalmologist performed all intravitreal injections aseptically at the temporal limbus through the eyeball's pars plana. All patients received IVC (10 mg/mL, 50 μL); using a 30-gauge needle. The interval between each injection was no more than 1mo.

OCT Evaluation Retinal imaging was conducted using a Spectralis OCT system (Heidelberg Engineering GmbH, Germany) across a 9 mm \times 7.5 mm area centered on the fovea. HEs are defined on OCT as the lesions size larger than 30 μm with the reflectivity resembling retinal pigment epithelium and the presence of back shadow. These HEs are predominantly located in the inner retinal layers, spanning from the nerve fiber layer to the outer nuclear layer. The measurement of HEs was performed using Image J software (version 1.53). OCT scans were imported into Image J, converted to 8-bit, and then sharpened to enhance clarity. Subsequently, relevant areas were selected for measurement. Assessors were blinded to the group assignments of participants to minimize bias in the evaluation of outcomes.

Reagents and Antibodies The Dil-Ox-LDL was purchased from Invitrogen (L34358; Carlsbad, CA, USA). The Ox-LDL and primary antibodies against anti-Ox-LDL were purchased from Yubo Biomed Technologies (Shanghai, China). Conbercept was purchased from Chengdu Kanghong

Table 1 Antibody information

Antibodies	Species origin	Source	Identifier
CD36	Rabbit	Huaan Biotechnology (China)	Cat# JJ2005
IL-6	Rabbit	Immunoway (USA)	Cat# YT5348
iNOS	Rabbit	Immunoway (USA)	Cat# YT3169
NF-κB	Rabbit	Proteintech (USA)	Cat# 10745-1-AP
PPARγ	Rabbit	Affinity (USA)	Cat# AF6284
VEGF-A	Rabbit	Proteintech (USA)	Cat# 19003-1-AP
VEGFR2	Rabbit	Zenbio (China)	Cat# 380984
p-VEGFR2	Rabbit	Cell Signaling Technology (USA)	Cat# 2487
β-actin	Rabbit	Servicebio (China)	Cat#15001
β-tubulin	Rabbit	Servicebio (China)	Cat#11017

CD36: Cluster of differentiation 36; IL-6: Interleukin-6; iNOS: Inducible nitric oxide synthase; NF-κB: Nuclear factor kappa-light-chain-enhancer of activated B cells; PPARγ: Peroxisome proliferator-activated receptor gamma; VEGF-A: Vascular endothelial growth factor A; p-VEGFR2: Phosphorylated vascular endothelial growth factor receptor 2.

Pharmaceutical Group Co., Ltd. (Sichuan Province, China). DMEM High Glucose Medium (SH30021.01B) was purchased from HyClone (Logan, UT, USA). CY3 goat anti-rabbit IgG (GB21303), FITC goat anti-mouse IgG (GB22301). The primers were synthesized from Sangon Biotech (Shanghai, China). Antibody information was listed in Table 1.

Rat Müller Cell Culture The transformed rat retinal Müller cell line (rMC-1) was generously provided by Sarthy from Northwestern University, located in Chicago, Illinois, USA. The cells were cultured in DMEM enriched with normal glucose (NG; 5.5 mmol/L) or high glucose (HG; 30 mmol/L) and supplemented with 10% fetal bovine serum (10099158; Gibco, Shanghai, China) and 1% penicillin/streptomycin (C0222; Beyotime Biotechnology). The cells were incubated at a temperature of 37°C and 5% CO₂ in a humidity-controlled incubator. Once the cells reached approximately 80% confluence in a 10-cm dish, they were divided into three groups (vehicle control, Ox-LDL, and Ox-LDL+conbercept) or four groups (control, HG, HG+Ox-LDL, and HG+Ox-LDL+conbercept). Two types of Ox-LDL were used in different experiments: 10 μg/mL Dil-Ox-LDL (ThermoFisher, USA) for immunofluorescence, flow cytometry and quantitative real-time polymerase chain reaction (qRT-PCR), and 10 μg/mL Ox-LDL (Yubo, Shanghai, China) for Western blot.

Cell Viability Assay Cell viability was assessed using the cell counting kit-8 (CCK-8; C0037; Beyotime Biotechnology). Cells were seeded in 96-well plates and treated with varying concentrations of conbercept (ranging from 10 to 500 μg/mL) for 24h. Post-treatment, 10 μL of CCK-8 solution was added to each well and incubated in the dark for 1h. Subsequently, the optical density was quantified using a microplate reader by measuring absorbance at 450 nm.

Immunofluorescence of Ox-LDL in rMC-1 Cells rMC-1 cells were incubated with Ox-LDL, either with or without

conbercept, for 24h. The cells were then fixed in cold methanol for 30min and blocked with 3% bovine serum albumin (BSA) in phosphate-buffered saline (PBS) for 1h. Subsequently, the cells were incubated overnight at 4°C with anti-Ox-LDL (1:100, rabbit) and glial fibrillary acidic protein (GFAP; 1:500, mouse). Next, after three successive 5-minute rinses in PBS, the cells were incubated for 2h at room temperature with the respective secondary antibodies (1:1000, anti-rabbit CY3; 1:1000, anti-mouse FITC). Dil-Ox-LDL was used in accordance with the manufacture's protocol. Then, the cells were further incubated with 4',6'-diamidino-2'-phenylindole (DAPI, 100 ng/mL) for 5min, followed by three washes (5min each wash). Finally, the slides were visualized with a confocal microscope (LSM 800; Zeiss Microsystems, Germany).

Reactive Oxygen Species Intracellular reactive oxygen species (ROS) levels were measured using the reactive oxygen species assay kit (Beyotime Biotechnology, China) according to the manufacturer's instructions. Briefly, rMC-1 cells were seeded in 24-well plates and divided into four groups: NG, HG, HG+Ox-LDL, and HG+Ox-LDL+conbercept. After 24h of treatment, cells were washed with PBS and incubated with 2',7'-dichlorodihydrofluorescein diacetate (DCFH-DA, 10 μmol/L) at 37°C for 30min in the dark. Following incubation, cells were washed three times with PBS to remove excess probe. Fluorescence intensity, indicative of ROS levels, was immediately measured using a fluorescence microscope (Zeiss, Germany) and quantified using Image J software (version 1.53). Experiments were performed in triplicate.

Protein Extraction and Western Blot The rMC-1 cells were incubated for 24h with Ox-LDL, in conditions with or without conbercept supplementation. Cells were lysed in protein extraction radioimmunoprecipitation assay (RIPA; P0013B; Beyotime Biotechnology) buffer on ice. Following a 15-second ultrasonication, the samples were chilled on ice for 30min prior

to centrifugation. Protein levels were then measured using the bicinchoninic acid (BCA) protein assay kit (A5586; Thermo Scientific, Shanghai, China). Identical protein quantities were separated on SDS-polyacrylamide gels and then electrophoretically transferred to nitrocellulose membranes. The membranes were incubated in 5% nonfat milk dissolved in PBS to block non-specific binding at room temperature for 1h. Following blocking, the membranes were incubated overnight at 4°C with primary antibodies against anti-Ox-LDL (1:1000, rabbit), vascular endothelial growth factor A (VEGF-A; 1:2000, rabbit), vascular endothelial growth factor receptor 2 (VEGFR2; 1:1000, rabbit), phosphorylated VEGFR2 (p-VEGFR2; 1:1000, rabbit), nuclear factor kappa-light-chain-enhancer of activated B cells (NF-κB; 1:1000, rabbit), interleukin-6 (IL-6; 1:1000, rabbit), inducible nitric oxide synthase (iNOS; 1:1000, rabbit), peroxisome proliferator-activated receptor gamma (PPAR-γ; 1:500, rabbit), cluster of differentiation 36 (CD36; 1:1000, rabbit), β-actin (1:5000) and β-tubulin (1:5000). Following three washes in 0.1% tris-buffered saline with Tween-20 (TBST), the membranes were exposed to the appropriate secondary antibodies (1:2000, anti-rabbit) at room temperature for 2h. Subsequently, they were washed three additional times with TBST. Detection of the bands was done using Chemi Doc™ Touch System (Bio-Rad). Immunoblots were visualized by enhanced chemiluminescence (ECL) and analyzed using Image J software version 1.53 (<http://imagej.nih.gov/ij/>).

Flow Cytometry Dil-Ox-LDL, either with or without conbercept, was added to the medium and incubated for 4h. After three 5-minute washes in PBS, adherent rMC-1 cells were collected, then digested with trypsin. The fluorescence of cells was analyzed with a flow cytometer (PE-A; Beckman CytoFLEX). Data were analyzed with FlowJo software (Tree Star Inc.).

Quantitative Real-Time Reverse Transcription Polymerase Chain Reaction The rMC-1 cells were treated with Ox-LDL or Ox-LDL+conbercept for 24h. The mRNA expression levels were analyzed by qRT-PCR (CXF96, Bio-Rad) using SYBR Green (208054, QIAGEN, Germany) based gene expression. In brief, adherent rMC-1 cells were lysed and the total RNA was extracted for cDNA synthesis (K16225, Thermo, USA). Levels of mRNA expressions were normalized by the intensity of glyceraldehyde 3-phosphate dehydrogenase (GAPDH). The data were expressed relative to the controls. The information for primers was provided in Table 2.

Statistical Analysis Data were expressed as mean±standard deviation (SD) and analyzed using pairwise *t*-tests. A *P*<0.05 was considered statistically significant. For data requiring statistical analysis, the experiments were repeated at least 3 times.

Table 2 Primer information for rats

Genes	Primers	Sequences (5'-3')
CD36	Forward	AGCTGCACCACATATCTACACA
	Reverse	AGAATGGATCTTTGTAACCCAC
GAPDH	Forward	GACATGCCGCCTGGAGAAAC
	Reverse	AGCCAGGATGCCCTTTAGT
LOX-1	Forward	CCACAAGACTGGATCTGGCAT
	Reverse	AGATAGGCAATTCTCCCGACT

LOX-1: Lectin-like oxidized low-density lipoprotein receptor-1; *CD36*: Cluster of differentiation 36; *GAPDH*: Glyceraldehyde-3-phosphate dehydrogenase.

RESULTS

Patient Characteristics and Effect of Anti-VEGF on HEs Reduction Twenty-one eyes from 17 patients with DME were retrospectively reviewed in this study. The participants included 10 females and 7 males, with an average age of 56.6±9.2y. In Figure 1A, the OCT image of a patient with DME exhibited a progressive fluid absorption in macula following an increasing number of IVC. Notably, there was a concurrent decrease in the size of HEs following the escalating frequency of IVC. This observation suggests the potential activation of Müller cells' phagocytic function, considering their anatomical localization within the INL. The areas of HEs were quantified in each patient following 3 consecutive injections (Figure 1B). The changes of HEs area were further normalized by the baseline to assess the reduction after each IVC (Figure 1C). Statistically, there was no significant change in the area of HEs between the baseline and the first follow-up, with measurements ranging from 1.39±1.41 to 1.38±1.3 mm² (*P*=0.938). However, a significant reduction was observed at the second and third follow-ups, with the HEs area measured at 0.77±0.9 mm² (*P*=0.021) and 0.45±0.66 mm² (*P*=0.002), respectively (Figure 1C).

rMC-1 Cells Phagocytosed Ox-LDL under HG Condition Under HG condition, confocal microscopy analysis revealed that Ox-LDL engulfment occurred in the cytoplasm of GFAP-labelled rMC-1 cells with close proximity to the nucleus (Figure 2A). Additionally, 2.5D reconstruction of the Dil-Ox-LDL signals demonstrated their localization near the nuclei (Figure 2B), confirming the occurrence of phagocytosis.

Conbercept Decreased rMC-1 Cells Viability in a Dose-Dependent Manner The viability of rMC-1 cells under HG conditions exhibited a dose-dependent response upon treatment with different concentrations of conbercept. As shown in Figure 2G, when treated with increasing concentrations of conbercept, the cell viability of the rMC-1 cells was observed to be 94.40% (10 μg/mL, *n*=3, *P*>0.05), 88.49% (50 μg/mL, *n*=3, *P*<0.05), 92.23% (100 μg/mL, *n*=3, *P*<0.05), 80.42% (300 μg/mL, *n*=3, *P*<0.01), and 70.76% (500 μg/mL, *n*=3, *P*<0.05) of the control, respectively. Considering that conbercept exhibits a

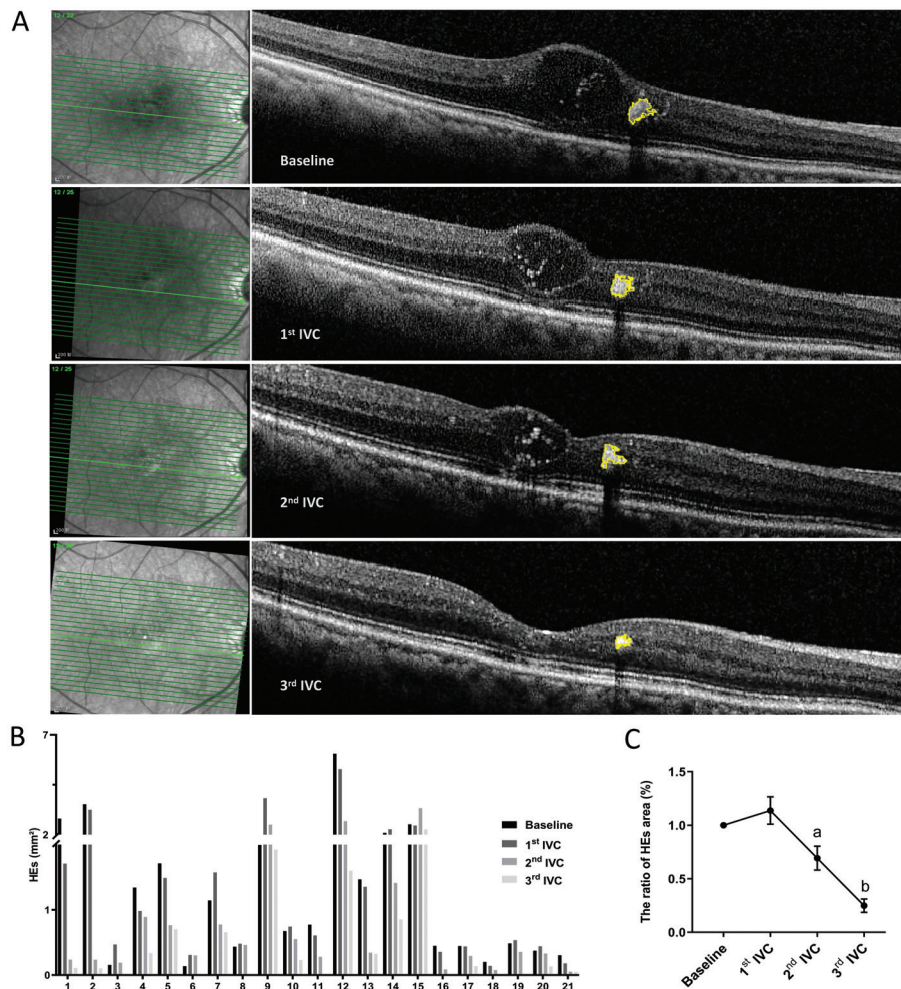


Figure 1 Alterations in the size of HEs among patients with DME following IVC treatment The HEs area showed minimal change after the first IVC but significantly decreased after the second and third IVCs. A: Representative images of the changes of HEs area in a patient at baseline and after each IVC; B: The quantitation of HEs area at baseline and after each IVC in all 21 eyes; C: The changes of HEs area were normalized by baseline after IVC in Figure B ($n=21$). Data are presented as mean \pm SD; ^a $P<0.05$, ^b $P<0.01$. HEs: Hard exudates; IVC: Intravitreal conbercept injection.

comparable and relatively modest (less than 12%) decline in rMC-1 cells viability within the concentration range of 10-100 $\mu\text{g/mL}$, with a notable increase in inhibition to 20% at 300 $\mu\text{g/mL}$, it can be inferred that the conbercept concentration range of 0-100 $\mu\text{g/mL}$ is relatively safe for rMC-1 cells. Consequently, we selected a treatment concentration of 100 $\mu\text{g/mL}$ for subsequent *in vitro* experiments.

Conbercept Significantly Enhanced the Phagocytosis of Ox-LDL by rMC-1 Cells To further verify the increased uptake of Ox-LDL by rMC-1 cells under HG conditions with or without conbercept, we employed immunofluorescence and Western blot to visualise and quantify the internalised amounts of Dil-Ox-LDL and Ox-LDL within the cells (Figure 2C-2F). The analysis showed that conbercept treatment led to a 23% increase ($n=3$, $P<0.05$; Figure 2C-2D) in intracellular Dil-Ox-LDL levels by immunofluorescence as well as a 22% increase ($n=3$, $P<0.05$) in Ox-LDL levels by Western blot (Figure 2E-2F). Additionally, flow cytometry analysis confirmed 21%

enhancement ($n=3$, $P<0.01$) in Dil-Ox-LDL uptake with conbercept treatment (Figure 2H-2I). These results indicated that conbercept could effectively enhance the phagocytotic activity of rMC-1 cells towards Ox-LDL under diabetic conditions. **Conbercept Activated PPAR γ -CD36 Axis in Müller Glia Through Inhibiting VEGF Pathway to Reduce Inflammation and Oxidative Stress** Western blot analysis demonstrated significant differences in protein expression between HG and NG group. In HG group, rMC-1 cells exhibited markedly elevated levels of VEGF-A and p-VEGFR2 ($P<0.05$ vs NG; Figure 3A and 3D). Concurrently, HG upregulated NF- κ B and its downstream inflammatory mediators, IL-6 and iNOS ($P<0.05$; Figure 3B and 3E). Conbercept treatment under HG conditions not only reduced VEGF-A ($P<0.05$) but also further suppressed p-VEGFR2 ($P<0.01$) and restored NF- κ B ($P<0.05$), IL-6 ($P<0.05$), and iNOS ($P<0.01$) expression to near-NG levels. Notably, PPAR γ protein, which was suppressed under HG, was robustly restored by conbercept

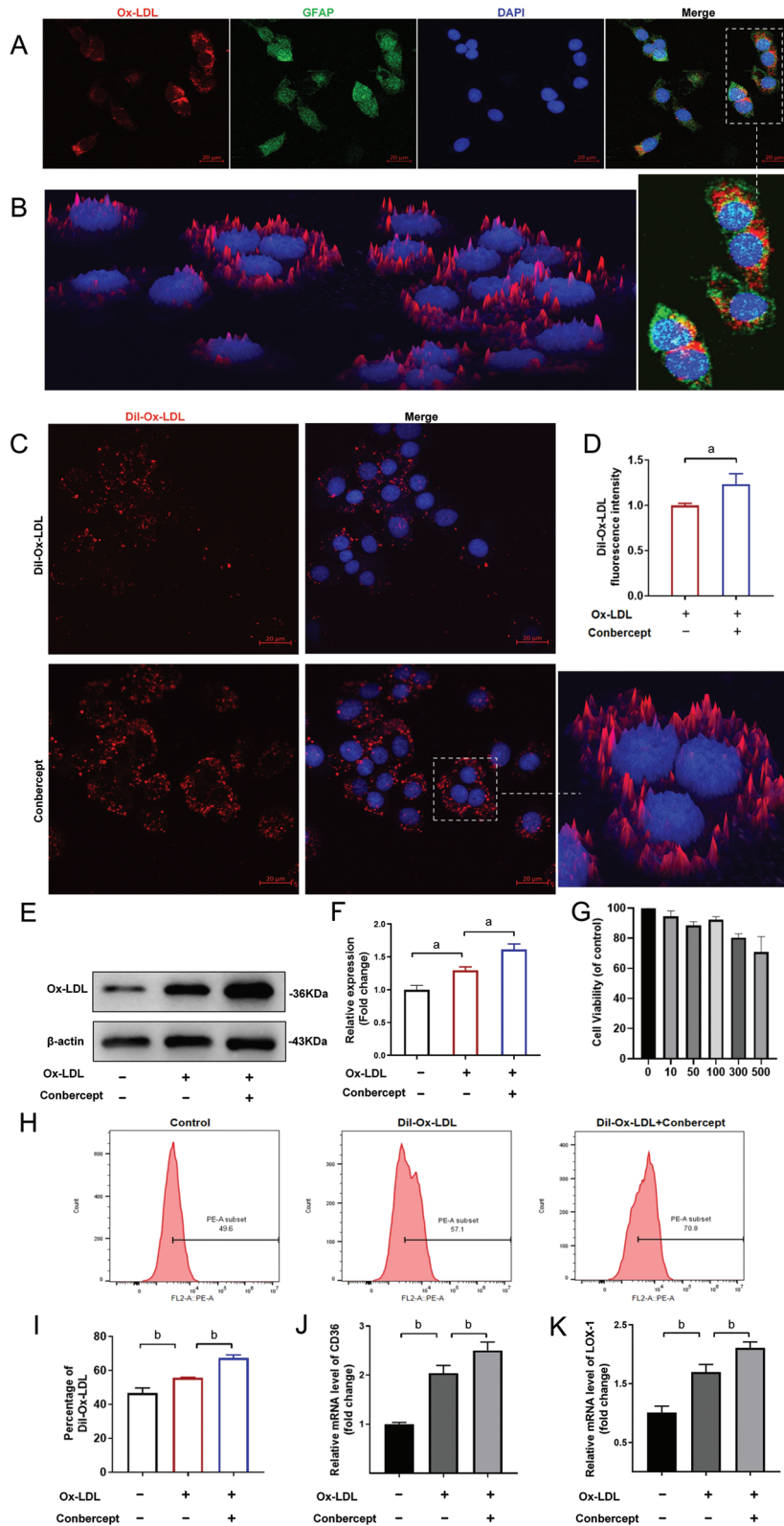


Figure 2 Conbercept enhances rMC-1 cells phagocytosis of Ox-LDL under HG conditions. A, B: Immunofluorescence staining after 24h of incubation showed co-localization of Ox-LDL (red) and GFAP (green), confirming uptake by rMC-1 cells; C, D: Confocal imaging revealed perinuclear accumulation of Dil-Ox-LDL in rMC-1 cells and quantitative analysis indicated that conbercept significantly increased the fluorescence intensity of Dil-Ox-LDL uptake; E, F: Western blot analysis showed elevated intracellular Ox-LDL levels in the Ox-LDL group compared to the control, with conbercept further enhancing this accumulation; H, I: Flow cytometry analysis confirmed that conbercept significantly promoted Dil-Ox-LDL uptake; G: The effect of conbercept on rMC-1 cells viability under high glucose conditions; J, K: qRT-PCR analysis revealed that Ox-LDL upregulated the expression of scavenger receptors CD36 and LOX-1, and conbercept further increased their mRNA expression levels. Scale bar: 20 μm. *n* = 3. ^a*P* < 0.05, ^b*P* < 0.01. rMC-1: Rat Müller cell line; Dil-Ox-LDL/Ox-LDL: Oxidized low-density lipoprotein; GFAP: Glial fibrillary acidic protein; CD36: Cluster of differentiation 36; LOX-1: Lectin-like oxidized low-density lipoprotein receptor-1.

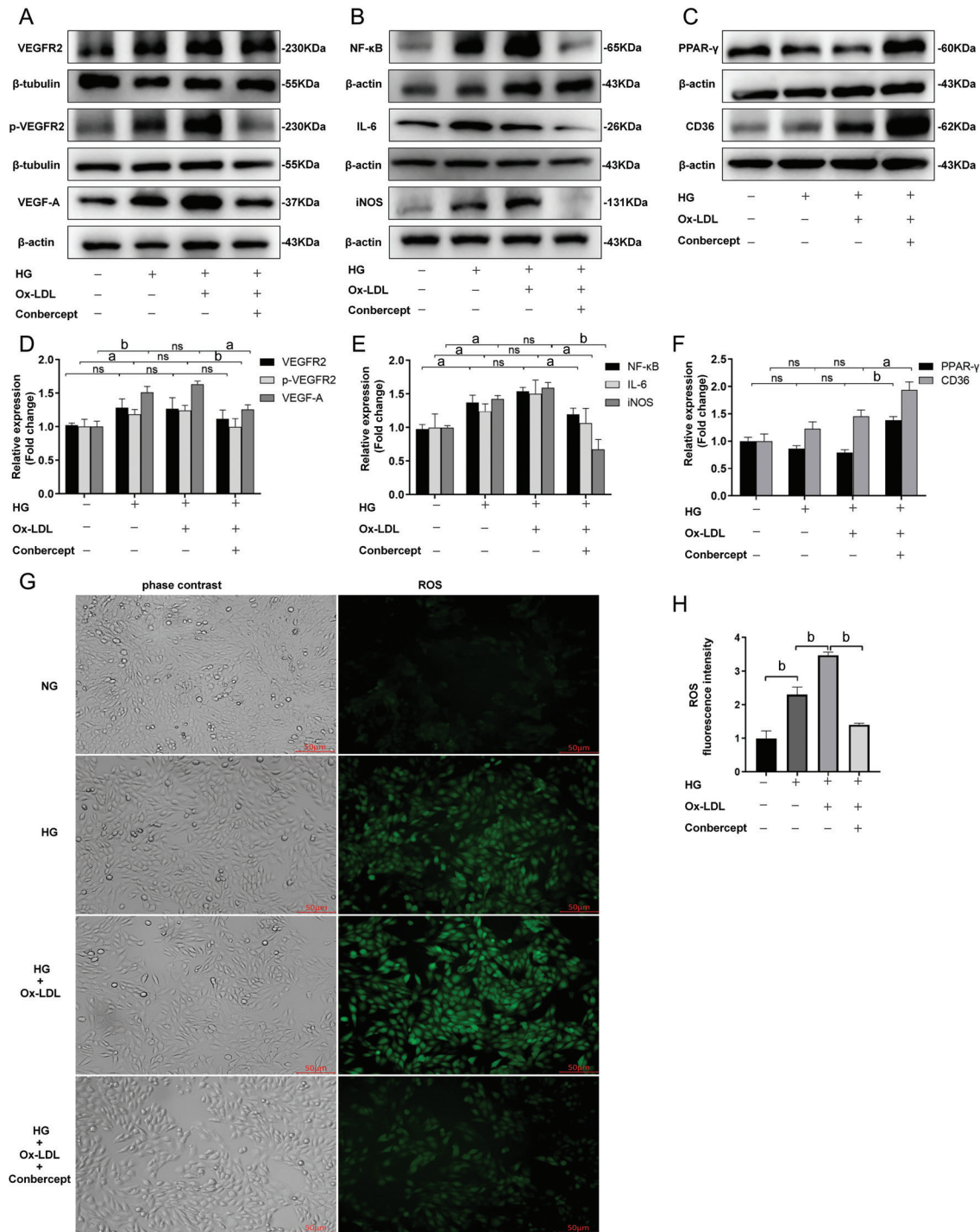


Figure 3 Under HG condition, conbercept suppresses VEGF signaling and inflammatory pathways to enhance lipid uptake in rMC-1 cells A-C: After 24h of incubation, the expressions of VEGFR2, p-VEGFR2, VEGF-A, NF-κB, IL-6, iNOS, PPAR-γ, and CD36 proteins were assessed by Western blot in the NG group, HG group, HG+Ox-LDL group, and HG+Ox-LDL+conbercept group; D-F: Quantification of the corresponding protein expression; G, H: Immunofluorescence of ROS in four groups, as well as the corresponding quantitative analysis. The measurements were performed at least three times. Scale bar: 50 μm. n=3. ^aP<0.05, ^bP<0.01. NG: Normal glucose; HG: High glucose; Ox-LDL: Oxidized low-density lipoprotein; VEGF-A: Vascular endothelial growth factor A; VEGFR2: Vascular endothelial growth factor receptor 2; p-VEGFR2: Phosphorylated VEGFR2; NF-κB: Nuclear factor kappa-light-chain-enhancer of activated B cells; IL-6: Interleukin-6; iNOS: Inducible nitric oxide synthase; PPARγ: Peroxisome proliferator-activated receptor gamma; CD36: Cluster of differentiation 36; ROS: Reactive oxygen species.

(*P*<0.01; Figure 3C and 3F). This recovery of PPARγ was accompanied by a significant increase in CD36 expression (*P*<0.05). qRT-PCR further confirmed that conbercept amplified Ox-LDL-induced upregulation of CD36 and LOX-1

mRNA (*P*<0.01; Figure 2J-2K). Immunofluorescence revealed that HG combined with Ox-LDL significantly elevated ROS levels compared to NG (*P*<0.01), an effect attenuated by conbercept treatment (*P*<0.01; Figure 3G-3H).

DISCUSSION

DR and DME are characterized by vascular dysfunction, lipid accumulation, and chronic inflammation, with HEs serving as a hallmark of retinal lipid deposition^[18]. Although anti-VEGF therapies like conbercept are widely used to reduce vascular leakage and edema^[19-21], their role in modulating Müller gliamediated lipid clearance remains underexplored. This study integrates clinical observations and *in vitro* experiments to elucidate a novel mechanism by which conbercept enhances Müller cell phagocytosis of Ox-LDL, thereby facilitating HEs resolution.

HEs formation results from increased vascular permeability due to lesions in the microvessels in the retina. Normally, the endothelial cells of retinal blood vessels form tight junctions that prevent plasma components from entering retinal tissue^[22]. However, in DR or DME, impaired vascular barrier function leads to the increased leakage of lipids and proteins from the blood into the parenchymal tissue of the retina. These leakages usually accumulate between the outer plexiform layer (OPL) and the INL of the retina because the anatomy and vascular supply of this region make it a reservoir for leakage^[23]. Specifically, the OPL is the synaptic region of neurons with a rich microvascular network, while the INL contains the nucleus of retinal cells. The structural characteristics of these layers lead to the easy deposition of exudates to form HEs.

Clinically, repeated IVCs markedly reduced the area of HEs in diabetic patients with DME, particularly after the third injection (Figure 1). This spatial correlation aligns with the anatomical localization of Müller cell somata, suggesting their direct involvement in HEs clearance. *In vitro* experiments further demonstrated that conbercept enhances the uptake of Ox-LDL by Müller cells under HG condition (Figure 2A-2I). Conbercept suppressed VEGF-A/VEGFR2 signaling and downstream inflammatory pathways^[24], leading to reduced NF- κ B activation and decreased expression of pro-inflammatory mediators (IL-6, iNOS)^[25], as well as diminished oxidative stress, evidenced by lower ROS levels (Figure 3). By inhibiting NF- κ B, conbercept alleviated its suppression on PPAR γ , a nuclear receptor essential for lipid homeostasis. This suppression is relieved through two primary mechanisms: competition for coactivators (*e.g.*, CBP/p300) and direct physical interaction (*e.g.*, PPAR γ binding to NF- κ B p65)^[26-29]. Furthermore, the reduction in inflammation and oxidative stress stabilized the intracellular environment, creating a conducive intracellular environment for PPAR γ recovery^[30]. The activation of PPAR γ and the subsequent increase in CD36 have been confirmed to enhance the protective role of microglial cells against retinal degenerative diseases^[31]. Our study demonstrates that the restoration of PPAR γ function

upregulated PPAR γ -CD36 signaling axis, which is critical for Ox-LDL internalization. PPAR γ promotes CD36 transcription, enabling the direct binding and phagocytosis of Ox-LDL^[32-33], thereby enhancing lipid clearance and accelerating the resolution of HEs. This mutual antagonism between NF- κ B and PPAR γ creates a feedback loop where reduced NF- κ B activity enhances PPAR γ function, and *vice versa*. Under diabetic conditions, NF- κ B activation promotes inflammation and oxidative stress, while PPAR γ activation enhances lipid clearance and anti-inflammatory responses. These findings highlight the potential of conbercept as a multifaceted therapeutic agent in DR/DME, addressing both vascular and metabolic pathologies.

The reduction of HEs following conbercept therapy holds significant clinical relevance. HEs are not merely bystanders but contributors to photoreceptor damage and vision loss^[34]. By enhancing Müller cell phagocytosis, conbercept may mitigate secondary retinal injury, complementing its anti-angiogenic effects. Moreover, the suppression of VEGF signaling and inflammation (Figure 3) aligns with its established role in stabilizing the blood-retinal barrier^[19]. However, our study uniquely links these vascular effects to cellular lipid metabolism, proposing a paradigm shift in understanding anti-VEGF therapies.

The phagocytic capacity of Müller glia has been increasingly recognized in retinal homeostasis, yet its role in DR remains controversial^[16-17,35]. Our findings resolve this ambiguity by demonstrating that Müller cells actively engulf Ox-LDL under hyperglycemia, with conbercept amplifying this process (Figure 2).

While this study provides valuable insights into the mechanisms by which conbercept enhances Müller cell phagocytosis and reduces HEs in DR, it has some limitations. First, the study primarily focused on PPAR γ -CD36 axis, but other lipid metabolism pathways (*e.g.*, ABCA1, LXR) may also play a role in HEs clearance. Future studies should explore the potential contributions of these pathways to conbercept's therapeutic effects. Second, although qRT-PCR and Western blot were used to assess changes in mRNA and protein expressions, the study did not investigate whether these changes involve epigenetic regulation (*e.g.*, DNA methylation, histone modifications). Third, while our findings highlight Müller glia as the primary mediators of HEs clearance under conbercept therapy, the potential interplay between Müller cells and retinal immune cells (*e.g.*, microglia or macrophages) warrants further investigation. For example, activated microglia may synergize with or antagonize Müller cell phagocytosis in diabetic retinas, a dynamic interaction not captured in our *in vitro* model. Addressing these limitations

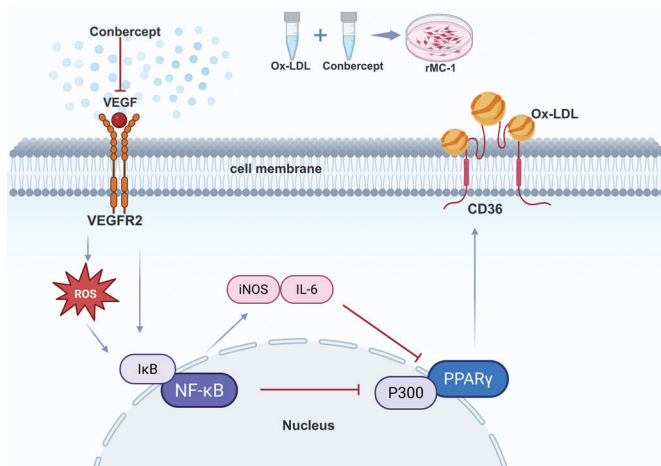


Figure 4 Schematic illustration of enhanced phagocytosis of HEs by Müller glia treated with conbercept The illustration was generated using BioRender.com. CD36: Cluster of differentiation 36; IκB: Inhibitor of kappa B; IL-6: Interleukin-6; iNOS: Inducible nitric oxide synthase; NF-κB: Nuclear factor kappa-light-chain-enhancer of activated B cells; Ox-LDL: Oxidized low-density lipoprotein; P300: E1A binding protein P300; PPARγ: Peroxisome proliferator-activated receptor gamma; ROS: Reactive oxygen species; rMC-1: Rat Müller cell line; VEGFR2: Vascular endothelial growth factor receptor 2; VEGF: Vascular endothelial growth factor.

spanning metabolic, epigenetic, and cellular cross-talk will provide a more comprehensive understanding of conbercept's therapeutic potential and guide the development of multifactorial treatment strategies for DR/DME. Moreover, complete patient data, including diabetes history, blood glucose control and concurrent medications during the study period, is of great importance, as these factors may influence the resolution of HEs in DME patients treated with conbercept.

In summary, conbercept demonstrates a multifaceted therapeutic profile in DR/DME, combining anti-VEGF, anti-inflammatory, and pro-phagocytic actions (Figure 4). By enhancing Müller glia-mediated Ox-LDL clearance through PPARγ-CD36 activation and suppressing VEGF-driven inflammation and oxidative stress, it addresses both vascular and metabolic pathologies. These findings expand the therapeutic scope of anti-VEGF agents and underscore the importance of targeting Müller cell dysfunction in DR/DME. Future research should focus on optimizing conbercept's lipid-modulating effects while ensuring retinal safety, paving the way for more holistic treatment strategies.

ACKNOWLEDGEMENTS

Availability of Data and Materials: All data generated or analyzed during this study are included in this published article.

Foundations: Supported by the National Natural Science Foundation of China (No.82171062; No.82301222; No.32201244).

Conflicts of Interest: Zhu YY, None; Qin SY, None; Xie H, None; Liu YP, None; Li XS, None; Zhang CY, None; Zhang YC, None; Zhang JF, None.

REFERENCES

- 1 Yanko L, Ungar H, Michaelson IC. The exudative lesions in diabetic retinopathy with special regard to the hard exudate. *Acta Ophthalmol (Copenh)* 1974;52(1):150-160.
- 2 Domalpally A, Ip MS, Ehrlich JS. Effects of intravitreal ranibizumab on retinal hard exudate in diabetic macular edema: findings from the RIDE and RISE phase III clinical trials. *Ophthalmology* 2015;122(4):779-786.
- 3 Tao Y, Jiang PF, Zhao Y, et al. Retrospective study of aflibercept in combination therapy for high-risk proliferative diabetic retinopathy and diabetic maculopathy. *Int Ophthalmol* 2021;41(6):2157-2165.
- 4 Shi R, Guo Z, Yang X, et al. Aggravation of retinal hard exudates after intravitreal anti-vascular endothelial growth factor therapy for cystoid macular edema and the risk factors: a retrospective study. *BMC Ophthalmol* 2022;22(1):92.
- 5 Igllicki M, González DP, Loewenstein A, et al. Next-generation anti-VEGF agents for diabetic macular oedema. *Eye (Lond)* 2022;36(2):273-277.
- 6 Wang Q, Li T, Wu Z, et al. Novel VEGF decoy receptor fusion protein conbercept targeting multiple VEGF isoforms provide remarkable anti-angiogenesis effect *in vivo*. *PLoS One* 2013;8(8):e70544.
- 7 Campa C. New anti-VEGF drugs in ophthalmology. *Curr Drug Targets* 2020;21(12):1194-1200.
- 8 Wang Y, Yao Y, Li R, et al. Different effects of anti-VEGF drugs (ranibizumab, aflibercept, conbercept) on autophagy and its effect on neovascularization in RF/6A cells. *Microvasc Res* 2021;138:104207.
- 9 Bringmann A, Pannicke T, Grosche J, et al. Müller cells in the healthy and diseased retina. *Prog Retin Eye Res* 2006;25(4):397-424.
- 10 Liu CY, Zhang XM, Yue HF, et al. The role of Müller cells in the formation and development of macular hole. *Zhonghua Yan Ke Za Zhi* 2023;59(11):948-953.
- 11 Munk MR, Somfai GM, de Smet MD, et al. The role of intravitreal corticosteroids in the treatment of DME: predictive OCT biomarkers. *Int J Mol Sci* 2022;23(14):7585.
- 12 Morales M, Findley AP, Mitchell DM. Intercellular contact and cargo transfer between Müller glia and to microglia precede apoptotic cell clearance in the developing retina. *Development* 2024;151(1):dev202407.
- 13 Zuo H, Han W, Wu K, et al. Prohibitin 2 deficiency in photoreceptors leads to progressive retinal degeneration and facilitated Müller glia engulfing microglia debris. *Exp Eye Res* 2024;244:109935.
- 14 Kinuthia UM, Wolf A, Langmann T. Microglia and inflammatory responses in diabetic retinopathy. *Front Immunol* 2020;11:564077.
- 15 Rathnasamy G, Foulds WS, Ling EG, et al. Retinal microglia—a key player in healthy and diseased retina. *Prog Neurobiol* 2019;173:18-40.
- 16 Nomura-Komoiike K, Saitoh F, Fujieda H. Phosphatidylserine recognition and Rac1 activation are required for Müller glia proliferation, gliosis and phagocytosis after retinal injury. *Sci Rep* 2020;10(1):1488.

- 17 Thiel WA, Blume ZI, Mitchell DM. Compensatory engulfment and Müller glia reactivity in the absence of microglia. *Glia* 2022;70(7):1402-1425.
- 18 Shukla UV, Tripathy K. Diabetic retinopathy. In: *StatPearls*. Treasure Island (FL): StatPearls Publishing; 2025.
- 19 RübSam A, Wernecke L, Rau S, et al. Behavior of SD-OCT detectable hyperreflective foci in diabetic macular edema patients after therapy with anti-VEGF agents and dexamethasone implants. *J Diabetes Res* 2021;2021:8820216.
- 20 Shen L, Zheng Y, Gao Z, et al. Efficacy and safety of intravitreal injection of conbercept for moderate to severe nonproliferative diabetic retinopathy. *Front Med (Lausanne)* 2024;11:1394358.
- 21 Si M, Tao Y, Zhang Z, et al. Retinal vein changes in patients with high-risk proliferative diabetic retinopathy treated with conbercept and panretinal photocoagulation co-therapy: a cohort study. *Front Endocrinol (Lausanne)* 2023;14:1218442.
- 22 O'Leary F, Campbell M. The blood–retina barrier in health and disease. *FEBS J* 2023;290(4):878-891.
- 23 Kuroiwa DAK, Malerbi FK, Regatieri CVS. New insights in resistant diabetic macular edema. *Ophthalmologica* 2021;244(6):485-494.
- 24 Cai S, Yang Q, Li X, et al. The efficacy and safety of aflibercept and conbercept in diabetic macular edema. *Drug Des Devel Ther* 2018;12:3471-3483.
- 25 Zhang M, Zhou M, Cai X, et al. VEGF promotes diabetic retinopathy by upregulating the PKC/ET/NF- κ B/ICAM-1 signaling pathway. *Eur J Histochem* 2022;66(4):3522.
- 26 Joharapurkar A, Patel V, Kshirsagar S, et al. Effect of dual PPAR- α γ agonist saroglitazar on diabetic retinopathy and oxygen-induced retinopathy. *Eur J Pharmacol* 2021;899:174032.
- 27 Pearson A, Koprivica M, Eisenbaum M, et al. PPAR γ activation ameliorates cognitive impairment and chronic microglial activation in the aftermath of r-mTBI. *J Neuroinflammation* 2024;21(1):194.
- 28 Blanquart C, Barbier O, Fruchart JC, et al. Peroxisome proliferator-activated receptors: regulation of transcriptional activities and roles in inflammation. *J Steroid Biochem Mol Biol* 2003;85(2-5):267-273.
- 29 Delerive P, De Bosscher K, Besnard S, et al. Peroxisome proliferator-activated receptor alpha negatively regulates the vascular inflammatory gene response by negative cross-talk with transcription factors NF-kappaB and AP-1. *J Biol Chem* 1999;274(45):32048-32054.
- 30 Xia JP, Liu SQ, Wang S. Intravitreal conbercept improves outcome of proliferative diabetic retinopathy through inhibiting inflammation and oxidative stress. *Life Sci* 2021;265:118795.
- 31 Zhou WC, He JC, Shen GY, et al. TREM2-dependent activation of microglial cell protects photoreceptor cell during retinal degeneration via PPAR γ and CD36. *Cell Death Dis* 2024;15(8):623.
- 32 Zhuang JL, Liu YY, Li ZZ, et al. Amentoflavone prevents ox-LDL-induced lipid accumulation by suppressing the PPAR γ /CD36 signal pathway. *Toxicol Appl Pharmacol* 2021;431:115733.
- 33 Wang T, Lu H. Ganoderic acid A inhibits ox-LDL-induced THP-1-derived macrophage inflammation and lipid deposition via Notch1/PPAR γ /CD36 signaling. *Adv Clin Exp Med* 2021;30(10):1031-1041.
- 34 Shen Y, Wang H, Fang J, et al. Novel insights into the mechanisms of hard exudate in diabetic retinopathy: Findings of serum lipidomic and metabolomics profiling. *Heliyon* 2023;9(4):e15123.
- 35 Colombo A, Dinkel L, Müller SA, et al. Loss of NPC1 enhances phagocytic uptake and impairs lipid trafficking in microglia. *Nat Commun* 2021;12(1):1158.